IEEE Photonics Journal
An IEEE Photonics Society Publication

Open Access

Experimental Investigations on TMI and IM-FWM in Distributed Side-Pumped Fiber Amplifier

Volume 12, Number 3, June 2020

Heng Chen
Jianqiu Cao
Zhihe Huang
Yuan Tian
Zhiyong Pan
Xiaolin Wang
Jinbao Chen

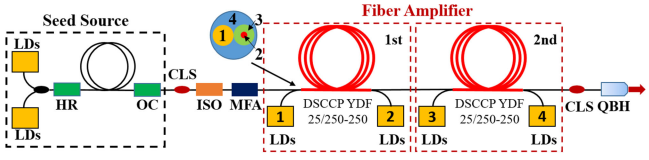

High power **distributed side-pumped fiber** amplifier with near-diffraction-limited beam quality

DOI: 10.1109/JPHOT.2020.2989242

IEEE photonics SOCIETY

IEEE

Experimental Investigations on TMI and IM-FWM in Distributed Side-Pumped Fiber Amplifier

Heng Chen,[1,2,3] **Jianqiu Cao,**[1,2,3] **Zhihe Huang,**[1,2,3] **Yuan Tian,**[1,2,3] **Zhiyong Pan,**[1,2,3] **Xiaolin Wang,**[1,2,3] **and Jinbao Chen**[1,2,3]

[1]College of Advanced Interdisciplinary Studies, National University of Defense Technology, Changsha 410073, China
[2]Hunan Provincial key Laboratory of High Energy Laser Technology, Changsha 410073, China
[3]Hunan Provincial Collaborative Innovation Center of High Power Fiber Laser, Changsha 410073, China

DOI:10.1109/JPHOT.2020.2989242
This work is licensed under a Creative Commons Attribution 4.0 License. For more information, see https://creativecommons.org/licenses/by/4.0/

Manuscript received January 30, 2020; revised April 16, 2020; accepted April 18, 2020. Date of publication April 20, 2020; date of current version May 26, 2020. This work was supported by the National Natural Science Foundation of China under Grant 61405249. Corresponding authors: Jianqiu Cao; Jinbao Chen (e-mail: jq_cao@126.com; kdchenjinbao@aliyun.com).

Abstract: The inter-modal four-wave mixing (IM-FWM) and transversal mode instabilities (TMI) are experimentally studied in high-power distributed side-pumped fiber amplifiers. To the best of our knowledge, we have made the first demonstration of TMI and IM-FWM which can be suppressed simultaneously by increasing the bending diameter. Besides, the experimental results show that the counter-pumping scheme is beneficial to suppress both of IM-FWM and TMI, when comparing with co-pumping scheme. Furthermore, these two effects cannot be observed when the M^2 factor is lower than 1.3, which can give a condition to estimate whether these two effects should be considered or not. The pertinent study can provide some guidance for understanding TMI and IM-FWM in the high-power fiber laser and amplifier.

Index Terms: Fiber laser, fiber nonlinear optics, laser amplifiers.

1. Introduction

High average power fiber lasers (HPFL) have experienced a rapidly progress in the power scalability thanks to the development of high brightness laser diodes, fiber component and special fiber fabrication technology [1]–[6]. The power extraction from a single ytterbium-doped fiber laser with the near-diffraction-limited beam quality has reached over 10 kW [5]. However, the power scaling of single-mode fiber lasers is still facing two challenges: transverse mode instabilities (TMI) and nonlinear effects (especially, the stimulated Raman scatting, SRS). Previous studies have revealed that one solution to the nonlinear effect limitation is to increase the mode field area of active fiber [6]. However, the large mode area (LMA) fiber is generally sensitive to thermal effects such as TMI which leads to a dynamical energy transfer between the fundamental mode and the high-order mode beyond a certain threshold, and then worsens the output beam quality.

Nowadays, a number of studies have been carried out to understand TMI in high-power fiber lasers [7]–[15]. Although its physical origin is still not so clear yet, a common accepted view is

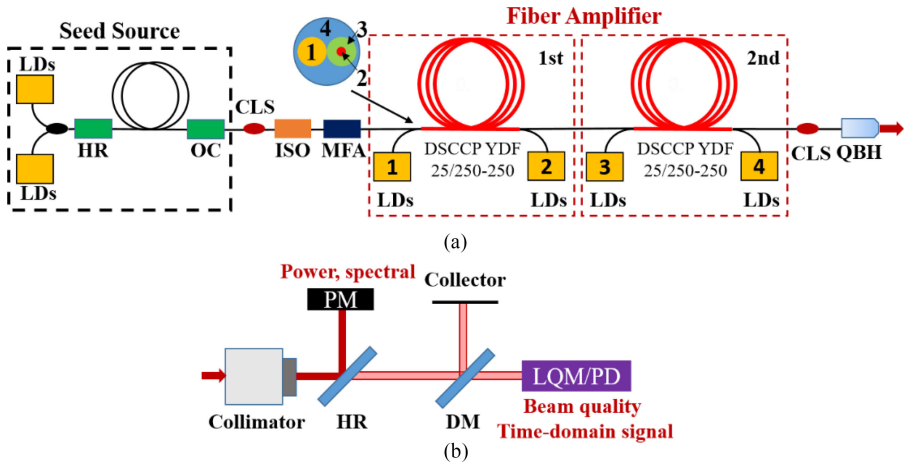

Fig. 1. (a) The schematic of the all-fiber distributed side-pumped fiber laser (inset is the cross section of DSCCP fiber). (b) The schematic of the measuring system (PM: power meter, LQM: Laser Quality Monitor, and PD: photodiode). After the output laser is collimated, it is reflected by a high reflecting mirror (HR $>$ 99.999%). The reflected light is used to measure power and collect spectra. The transmitted light passes through a dichroic mirror (DM) for beam quality measurement and temporal characteristics measurement.

that TMI is triggered by the thermal gratings which are induced by the interference pattern of fundamental mode (generally the LP_{01} mode) and high-order modes (generally the LP_{11} mode). Refs. [8], [9] revealed that a small frequency shift (about kHz) between the fundamental and high-order modes should be indispensable for the presence of TMI. Some measures for improving the TMI threshold (i.e., the output power corresponding to the presence of TMI) have been presented such as increasing the power of single-mode seed light [10], [11], increasing the linewidth of seed light [12], [13], increasing the loss of high-order modes (e.g., realized by coiling fiber [14], [15]), optimizing the doping of the core [11], [16], shifting the pump or signal wavelength [17], [18] and so on.

Besides, there is another effect known as the inter-modal four-wave mixing (IM-FWM) which has also attached attention recently because of the wavelength beam combining (WBC) application of fiber lasers [19]. Different from the monotonously spectral broadening induced by the self-phase modulation (SPM) [20]–[22], IM-FWM can generally induce a pair of spectral side lobes (corresponding to the phase matching between two modes) which is undesirable in the WBC application [19], [22]. Although IM-FWM has been substantially studied in the passive fiber [23], [24], pertinent studies in the active fiber or fiber laser are not so rich. In Refs. [25]–[27], IM-FWM was observed without detailed discussions. Refs. [2], [19] studied the frequency shift of side lobes induced by IM-FWM based on the phase-matching condition. It was also demonstrated that IM-FWM can be suppressed in two-mode fiber by decreasing the coiling diameter [19].

However, in few-mode fiber, the effective area drops and the benefit of larger core size for larger mode area disappears when the bending diameter decreases [28]. Thus, there is an interesting issue, i.e., how to suppress TMI and IM-FWM simultaneously in the few-mode fiber. In this paper, experimental studies are carried out to simultaneously investigate both of these two effects with the help of a distributed side-pumped fiber amplifier. The impact of the bending diameter and pumping scheme on IM-FWM and TMI are studied in experiments.

2. Experimental Setup

The experimental studies are based on a distributed side-pumped fiber amplifier (see Fig. 1). Here, the distributed side-coupled cladding-pumped (DSCCP) fiber [29], [30] (also known as GTWave fiber [31], [32], multi clad fiber [33] and multi-element first cladding fiber [34]) is used as the active

fiber and its configuration is given as the inset of Fig. 1(a). The DSCCP fiber consists of one pump fiber and one signal fiber. Core 1 is the core of pump fiber and Core 2 is the core of signal fiber. Cladding 3 is the inner-cladding of signal fiber which is physically separated but optically contacted with Core 1. Cladding 4 acts as both the cladding of pump fiber and the outer-cladding of signal fiber. Here, the DSCCP fiber is utilized based on the following considerations: the first one is that the cores of pump and signal fiber are separated from each other in the DSCCP fiber, which can minimize the effect of pump light injection on the propagation of signal light without tapering section (and thus the transverse modes or beam quality of the fiber amplifier). The second one is that the pumping scheme can be easily switching between counter-, bi-direction and co-pumping configurations.

The amplifier consists of two sub-amplifiers where a 15-m long DSCCP YDF is used in each sub-amplifier to ensure a full absorption of pump light. As shown in the inset of Fig. 1(a), the diameters of core 1 and inner-cladding 3 are both 250 μm, core 2 has a diameter of 25-μm diameter with a $\sim$0.065 numerical aperture (NA) and the diameter of outer cladding 4 is 650 μm. Pump light is supplied by four wavelength-stabilized 976-nm laser diodes (LDs, the central wavelength is 976 $\pm$ 0.5nm) via four pump fiber ends, then the pump light gradually couples into the inner-cladding of signal fiber in form of the evanescent wave. The smallest coiling diameter of the active fiber in the amplifier is 30 cm.

To test these two sub-amplifiers, a home-made single-mode seed source is used. The seed is composed of a pair of fiber Bragg gratings (FBG) centered at the wavelength of $\sim$1080 nm (the 3-dB spectral bandwidths is 2 nm and 1 nm, respectively), and $\sim$13-m double cladding ytterbium-doped fiber (YDF) with a core/inner-cladding diameter of 10/130 μm. The NA of active core is 0.07, which can guarantee the single mode operation. The laser oscillator is co-pumped by fiber-pigtailed 976-nm LDs through a 3 $\times$ 1 pump combiner. Between the amplifier and the seed source, a cladding light stripper (CLS) is utilized to strip out the residual pump light and the signal light propagating in the fiber cladding. An isolator (ISO) is incorporated to protect the seed laser source from the backward propagation light. Besides, a mode field adaptor (MFA) is employed to keep mode field diameter matched with low fundamental mode loss and minimal degradation of beam quality. The core/inner-cladding diameter of input fiber is 10/130 μm and that of output fiber is 25/250 μm, respectively. Then, about 45-W output power can be produced by the seed source.

A quartz block header (QBH) with 9-m long passive fiber is spliced to the output ports to eliminate probable harmful feedbacks. All the components of fiber laser systems are cooled by a heat sink to keep an appropriate working temperature. An optical spectrum analyzer is used to measure the spectrum of output laser. The beam quality and beam profile is measured by the Laser Quality Monitor. Besides, An InGaAs photodiode (PD, 150-MHz, 700-1800 nm), protected by a 1.5-mm diameter pinhole, is placed at the center of collimated light path for TMI monitoring.

3. Results and Discussions

3.1 IM-FWM and TMI in the Bi-Directional Side-Pumped Amplifier

Because the mode property of seed light is of great importance for study IM-FWM and TMI in the amplifier, the beam quality output from the MFA is firstly measured. It is found that the M^2 factor is 1.08, which means that the single-mode operation is well maintained when the seed light passes through the MFA. Then, the spectrum of seed source is also measured and the pertinent results are given in the inset of Fig. 2(b). It can be seen that the central wavelength is about 1079.8 nm with the full width at half-maximum (FWHM) of 0.18 nm. After that, the output properties is measured when the seed light passes through the cold-cavity (i.e., with no pump power) of the fiber amplifier. It is found that 38-W signal light can be output from the cold-cavity of amplifier when 45-W seed light is launched, and no obvious variation of spectrum is observed (i.e., centered at 1079.8 nm with 0.18-nm FWHM). Besides, the output beam quality is also measured and the pertinent M^2 factor is still 1.08 $\pm$ 0.01, which means that the cold-cavity of the fiber amplifier should have a negligible

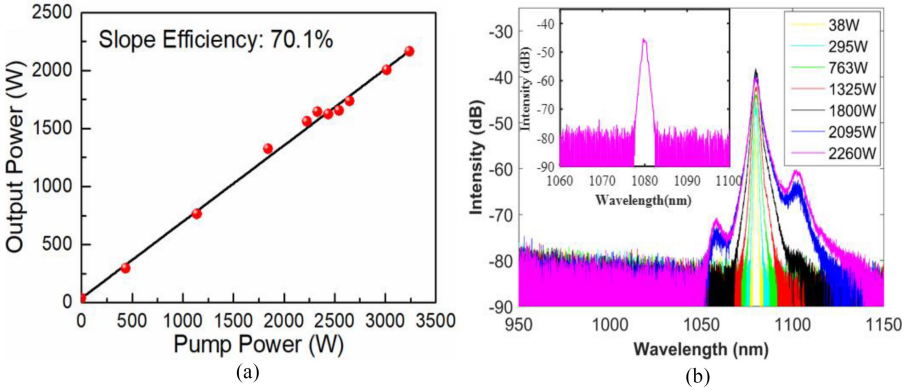

Fig. 2. (a) The laser output power versus the pump power and (b) the spectra of signal light at different output power (the seed spectrum is given as the inset).

TABLE 1
The propagation constant in different wavelength and different fiber mode

$\beta(\lambda_i,LP_{mn})$	$\beta(\lambda_i,LP_{01})/m^{-1}$	$\beta(\lambda_i,LP_{11})/m^{-1}$
λ_1=1079.8 nm	8437827.174	8435725.681
λ_2=1057.8 nm	8619849.094	8617768.677
λ_3=1101.8 nm	8255843.049	8253720.644

effect on the single-mode propagation of seed light although 30-cm coiling diameter is used in our experiments.

Then, four LDs are started and the pump light is injected into Port 1-4 (see Fig. 1a), which makes these two sub-amplifiers bi-directionally pumped and the pump power injected into each port is almost the same. The variations of output properties are measured with the increment of pump power and the results are given in Fig. 2(a). It can be found that the slope efficiency of the increment of output power is about 70.1%, and with the 3.24-kW total pump power, about 2.26-kW output power can be obtained. It can also be seen that the linear increment of output power is not maintained when the pump power varies from 2227 W to 2544 W, and the output power is even slightly dropped when the pump power varies from 2332 W to 2438 W.

We also measure the output spectrum of fiber amplifier which is given in Fig. 2(b). It can be seen that although the central wavelength of signal peak is still around 1079.8 nm, but two side-lobes with the central wavelengths of 1057.8 nm (anti-Stokes) and 1102.1 nm (Stokes) are present in the spectrum when the output power is larger than 1800 W. By calculating the propagation constant of transverse mode according to the configuration of active core (see Table 1), it can be known that the phase-matching condition [2], [19], [22] of IM-FWM can be satisfied by the LP_{01} and LP_{11} modes at these three wavelengths because

$$\beta(\lambda_2,\ LP_{01}) + \beta(\lambda_3,\ LP_{11}) = \beta(\lambda_1,\ LP_{01}) + \beta(\lambda_1,\ LP_{11}) \quad (1)$$

$$\beta(\lambda_2,\ LP_{11}) + \beta(\lambda_3,\ LP_{01}) = \beta(\lambda_1,\ LP_{01}) + \beta(\lambda_1,\ LP_{11}) \quad (2)$$

Thus, we can conclude that these two side-lobes in the output spectrum is induced by the IM-FWM [22]. In spite of that, Fig. 2(b) also shows that the Stokes side-lobe is stronger than the anti-Stokes side-lobe, which may mean that the gain around 1102.1 nm should be larger than that around 1057.8 nm in the fiber amplifier.

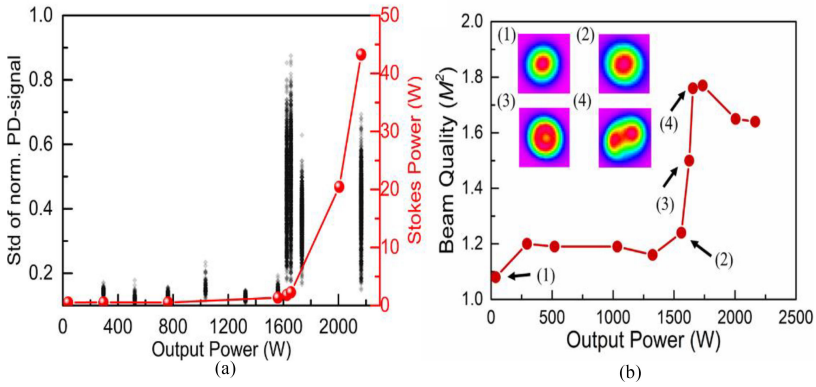

Fig. 3. (a) The standard deviation of normalized PD-signal (STD-PD) versus output power (black dots, left axes); the Stokes power as a function of the output power (red dots, right axes). (b) The beam quality of the output laser versus the output power, the inset (1) shows the beam profile of the seed light that passes through amplifiers without pump power, the insets (2)–(4) illustrate the beam profile for stable (2) and unstable (3 and 4) mode operation.

To measure the threshold of IM-FWM, we measure the output spectrum with a smaller step between the 1325-W and 1800-W output power and estimate the power of Stokes side-lobe by integrating the output spectrum, because both Stokes light and signal light are output from the core. The pertinent results are given as the red line of Fig. 3(a). It can be seen that Stokes power grows slowly with the increment of output power from 38 W to 1625 W. Then, the threshold-like onset of IM-FWM can be clearly observed as a sudden increase of Stokes power from 0.9 W to 3.3 W at the output power of 1645 W. It means that the IM-FWM should be present when the output power is larger than 1625 W, and thus, the threshold of IM-FWM should be 1625-W. It can also be seen that the drop of output power (see Fig. 2(a)) is just present when the output power reaches to around 1645 W. It is implied that the drop of output power should be caused by the presence of IM-FWM which will induce the side-lobes with the gain lower than the single peak [35].

The beam quality of output laser is also measured, and the results are given in Fig. 3(b). Fig. 3(b) shows the M^2 factor is gradually elevated from 1.08 to 1.24 with the increment of output power from 38 W to 1625 W, which means that the high-order mode becomes stronger with the increment of pump power. The enhancement of high-order mode can be induced by the transverse hole-burning effect [36]. In spite of that, the beam profile keeps a stable fundamental-mode-like image and no TMI is observed when the output power is lower than 1625 W. Then, when the output power is further increased, the M^2 experiences a sharp increase from 1.24 to 1.50 and the output beam becomes unstable in the mode content. It is implied that TMI should be present (a single frame is shown in the inset (3) of Fig. 3(a)).

In order to estimate the threshold of TMI, the PD signal at different power levels is recorded and the standard deviation of normalized PD-signal (STD-PD) is given as the black dots in Fig. 3(a) [1], [7]. It can be seen that the absolute values of STD-PD become much more dispersive when the output power is larger than 1625 W, which means that the threshold of TMI should be around 1625 W.

Then, an interesting result can be obtained from Fig. 3(a), i.e., both the TMI and IM-FWM can be observed when the output power is larger than the same value 1625 W. In other word, the TMI and IM-FWM share the same threshold in our fiber amplifier. To the best of our knowledge, this is the first time such a result is obtained in experiment and the pertinent origin is still not clear. In order to understand the observation, more experiments are carried out.

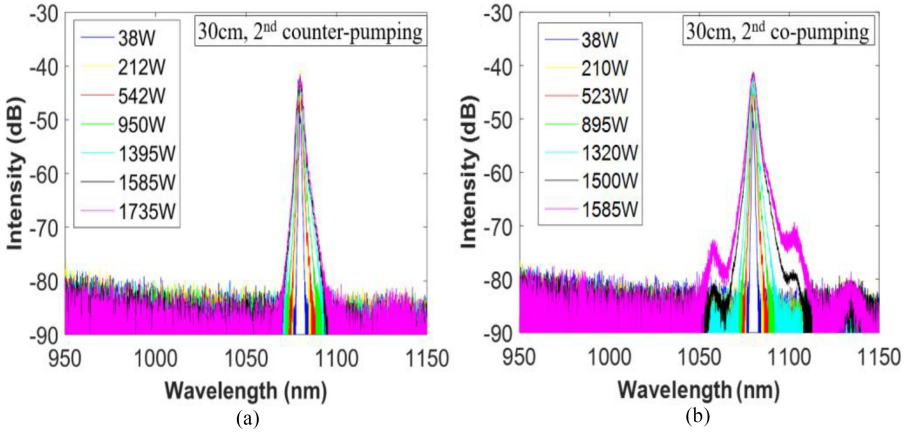

Fig. 4. The output spectra in the counter-and the co-pumping scheme are given in (a) and (b), respectively. IM-FWM is only observed in the co-pumping case (b).

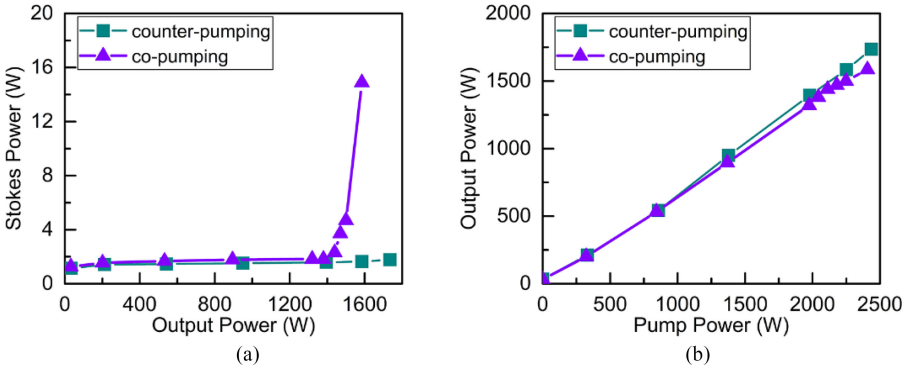

Fig. 5. (a) The evolution of Stokes power in the counter- (turquoise squares) and the co-pumping schemes (purple triangles) and (b) the output power versus the pump power in the counter-and the co-pumping schemes.

3.2 IM-FWM and TMI Under Different Pumping Configuration

In above subsection, two sub-amplifiers are evenly bi-directional pumped. In this section, the effects of different pumping schemes will be investigated experimentally. Note that the TMI and IM-TMI can only happen when the output power is high enough, they should present in the 2nd sub-amplifier. Thus, we firstly vary the pumping scheme of 2nd sub-amplifier while keep the 1st sub-amplifier is bi-directionally pumped (or the pump power is not high enough for TMI and IM-FWM. Actually, the effect of varying pumping scheme of 1st sub-amplifier is negligible, which will be demonstrated in the Section 3.3). The co-pumping and counter-pumping schemes are realized by shutting down one LD in the 2nd sub-amplifier.

The spectra corresponding to the co-and counter-pumping schemes of 2nd sub-amplifier are given in Fig. 4. IM-FWM is only observed in the co-pumping case in Fig. 4(b), which means that counter-pumping case has higher IM-FWM threshold compared with the co-pumping one. Then, the Stokes power is calculated to estimate the IM-FWM threshold. As shown in Fig. 5(a), the Stokes power remains unchanged with the increment of pump power in the counter-pumping case, while Stokes power increases rapidly beyond the output power of 1440 W in the co-pumping case. Thus, the IM-FWM threshold of the co-pumping case should be about 1440-W in our experiments. It is also implied that the IM-FWM threshold should be larger than 1735- W in the counter-pumping scheme. When comparing the IM-FWM thresholds among co-, counter-and bi-directional pumping cases, it can be known that the threshold of IM-FWM is lowest in the co-pumping case, higher in

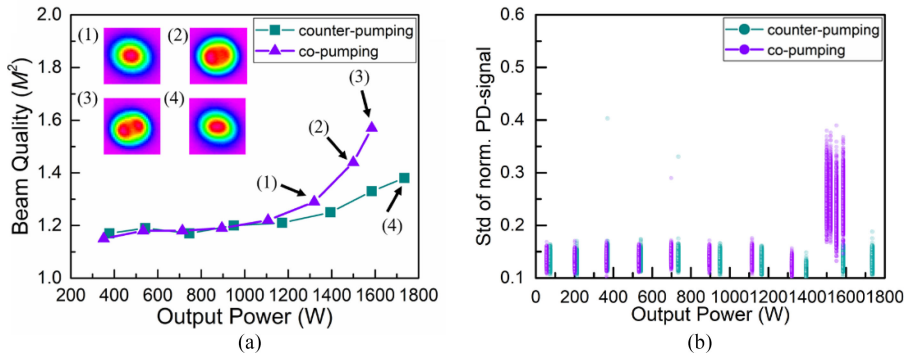

Fig. 6. (a) Purple triangles show the evolution of the beam quality in the co-pumping schemes, the insets (1)–(3) illustrate the beam profile for stable (1) and unstable (2/3) mode operation. Turquoise squares show the beam quality in the counter-pumping scheme, the inset (4) shows the beam profile at the maximum output power; (b) the evolution of the STD-PD in counter- (turquoise dots) and co-pumping (purple dots) schemes.

the bi-directional pumping case with the result given in Fig. 3(a), and the highest in the counter-pumping case. It is implied that the counter-pumping scheme is most beneficial to suppress the IM-FWM. Actually, The power variation and heat load distribution along the fiber are different for co- and counter-pumping cases, and the counter pumping case has a lower average signal intensity [38], [39] and a shorter interaction length which can increase the IM-FWM threshold [22]. Thus, it can be inferred that the IM-FWM threshold will be different at different ratio between co- and counter- pumping. Besides, a small SRS peak is also observed in the co-pumping case, which is reasonable because SRS is the most serious in the co-pumping scheme [37]–[39]. The plots of output power are given in Fig. 5(b) which shows that the slope efficiency of counter-pumping case (about 70.9%) is slightly higher than that of co-pumping one (about 67.0%).

Then, we measure the threshold of TMI corresponding to co- and counter-pumping cases. Fig. 6(a) gives the variation of beam quality. It can be found that the M^2 factor of co-pumping case becomes larger than that of counter-pumping one when the output power is larger than 1080 W. It is implied that more high-order mode is induced in the co-pumping case with the increment of output power. Fig. 6(b) gives the variation of STD-PD with the output power. It can be found that a sudden increment of STD-PD is present when the output power reaches to 1500 W, which implies the present of TMI with the threshold of 1500 W. In spite of that, such a variation of STD-PD cannot be observed in the case of counter-pumping case which means that no TMI is present with the 1735-W output power. Thus, the threshold of TMI of counter-pumping case should be larger than 1735 W. By comparing with the bi-directional pumping case shown in Fig. 3 (i.e., the threshold is 1625 W), it can be known that the counter-pumping case is the most beneficial, while the co-pumping one is the least beneficial to suppress the TMI in the fiber amplifier. These results are consistent with [40], [41], compared with co-pumping case, the counter-pumping case has lower upper state populations, which can increase the TMI threshold. By comparing Figs. 5(a) and 6, it can also be seen that the threshold of TMI and IM-FWM are also very close to each other in the co-pumping case, which implies that the pumping scheme only has a negligible effect on the similarity of two thresholds.

3.3 IM-FWM and TMI Under Different Bending Diameter

Besides the pumping scheme, another factor affecting TMI and IM-FWM is the bending diameter. Nowadays, majority of studies were carried out to show that both the TMI and IM-FWM can be suppressed by the reduction of bending diameter which can enhance the loss of high-order modes [14], [15]. However, considering the bend-induced coupling will be relieved with the increment of bending diameter [42], [43], it is interesting how these two thresholds will be varied by increasing

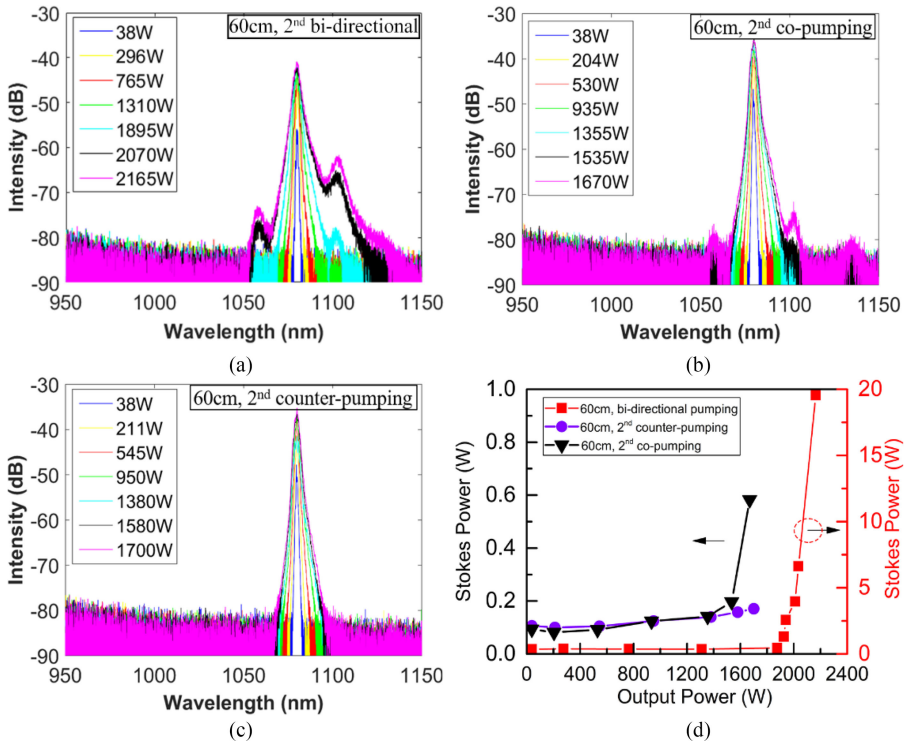

Fig. 7. The output spectra of the bi-directional, the co- and the counter-pumping in the 2nd sub-amplifier is shown in (a)–(c), respectively. (d) Stokes power versus the output power at different pumping scheme.

the bending diameter. Therefore, the minimum bending diameter of the DSCCP fiber is increased from 30 cm to 60 cm in experiments and the pertinent results will be given in the following parts.

Firstly, the output spectra of amplifier with various pump schemes (e.g., bi-directional, co- and counter-pumping of 2nd sub-amplifier) are measured. The 2nd sub-amplifier is also evenly pumped in bi-directional pumping case. IM-FWM can be observed in bi-directional case (Fig. 7(a)) and the co-pumping case (Fig. 7(b)), but not in counter-pumping case (Fig. 7(c)). By estimating the threshold of IM-FWM (see Fig. 7(d)), it can be found that the thresholds are about 1535 W and 1875 W corresponding to the co- and bi-directional pumping case, respectively. It is pity that the threshold corresponding to the counter-pumping case is not obtained because of the limitation of the pump power. In spite of that, we can know that it should be larger than 1700 W. Thus, the co-pumping case is also the worst one for suppressing IM-FWM. However, by comparing these results in the case of 30-cm bending diameter (see Figs. 3(a) and 5(a)), it can be seen that both the thresholds of co- and bi-directional pumping cases are obviously larger than those obtained with the 30-cm bending diameter, which means that the IM-FWM threshold can also be suppressed by increasing the bend diameter when the bending diameter is larger than 30 cm. To the best of our knowledge, this is the first demonstration on the positive effect of increasing the bending diameter on the suppression of IM-FWM. Such a result may be induced by the bending-dependent mode coupling which can enhance the high-order mode [42]–[45], if the bending diameter is not small enough to loss the high-order mode.

The TMI threshold are also measured with the results given in Fig. 8(a). It can be found that the TMI threshold corresponding to the bi-directional pumping case is about 2010 W, and the thresholds corresponding to the other two pumping cases are not obtained because of the limitation of pump power. In spite of that, it can be found that the M^2 factor for the co-pumping case becomes larger than that for the counter-pumping case when the output power is larger than 1460 W, which

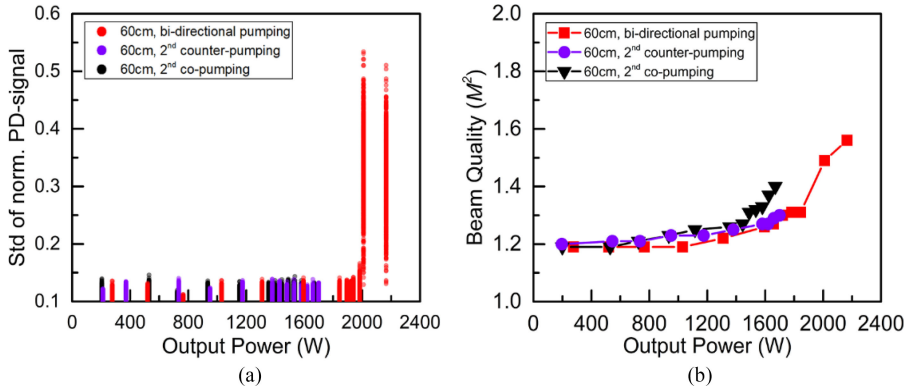

Fig. 8. (a) The evolution of the STD-PD in the bi-directional (red dots), counter- (purple dots) and co-pumping (black dots) schemes and (b) the evolution of the beam quality in the bi-directional (red squares), counter- (purple dots) and co-pumping (black triangles) schemes.

implies again that the counter-pumping case is more beneficial to suppress the TMI than the co-pumping one. By comparing with the results in the case of 30-cm bending diameter, it can be seen that the threshold of TMI is elevated by the increment of bending diameter, which may also be induced by the enhancement of high-order mode caused by the bending-dependent mode coupling.

Then, we compare the threshold of IM-FWM with that of TMI in the case of 60-cm bending diameter. It can be found that they are not so similar as the case of 30-cm bending diameter. Two thresholds of IM-FWM (1535 W and 1875 W corresponding to the co- and bi-directional pumping case, respectively) are both smaller than those of TMI (more than 1670 W and 2010 W), which means that the IM-FWM should be more easily produced than the TMI in the fiber amplifier. It is also implied that the threshold similarity of two effects cannot be maintained with the variation of bending-diameter. Some more discussions will be given in the following section.

We also examine the effect of pumping scheme variation of 1st sub-amplifier, and the pertinent results are given in Fig. 9. It can be seen that the threshold of IM-FWM can only be obtained (about 1650 W) with the co-pumping scheme, which is also obviously larger than the value (about 1530 W) with the 2nd sub-amplifier co-pumped. It is implied that the effect of pumping scheme variation of 1st sub-amplifier should be weaker than that of 2nd sub-amplifier. This is also the reason why we focus our investigation on the pumping variation of 2nd sub-amplifier.

3.4 Discussion

It should be noted that the Ref. [1] came to a different conclusion, about the correlation between the TMI threshold and the fiber bending diameter, from our results. In the Ref. [1], a commercial YDF with a core/clad diameter of 20/400 μm and a numerical aperture (NA) of 0.06 was used in the amplifier stage. The TMI threshold was increased with the bending diameter from 60 cm to 30 cm, and the TMI threshold was rising much stronger for increasing bending. However, the core/clad diameter of signal fiber was 25/250 μm with a core NA of 0.065 in our experiments, and the TMI got relieved when increasing bending diameter from 30 cm to 60cm. Besides, the similar results have been reported in the Ref. [43] without specific physical explanations.

This contradiction can be understood as follow: for the two-mode fiber in the Ref. [1], the V-value was 3.5431 which means that it only supports LP_{01} and LP_{11} modes. Due to the bend-dependent modal loss of LP_{11} mode is high enough [14], [46], which means that the LP_{01} mode has an advantage in gain competition with LP_{11} mode when bending diameter is decreasing. Even when the bending diameter ranged from $\sim$11 cm to $\sim$17 cm, the bend losses of LP_{01} ($<$0.1 dB/m) and LP_{11} ($>$10 dB/m) fitted the criteria of SM operation conditions [28]. Thus, the TMI threshold rose with the decrease of bending diameter. However, for the few-mode fiber in our experiments,

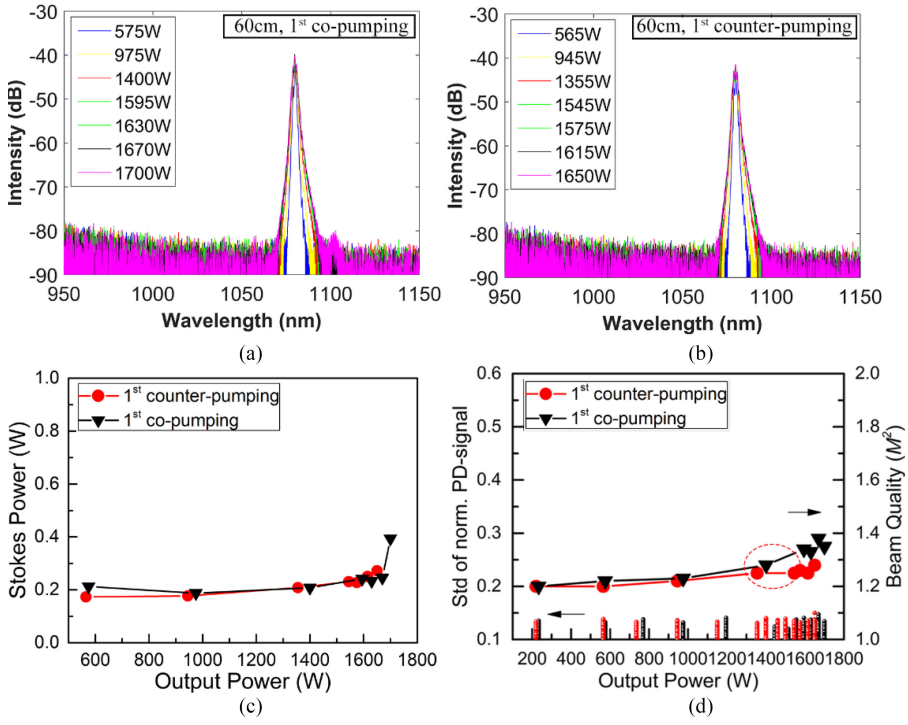

Fig. 9. (a) The output spectra of the 1st sub-amplifier in the co- and the counter-pumping scheme is given in (a) and (b), respectively. (c) The corresponding Stokes power versus the output power in the co- (red dots) and the counter-pumping (black triangles) scheme. (d) The evolution of the STD-PD in co- and counter-pumping schemes (left axis), the evolution of the beam quality in counter-and co-pumping schemes (right axis).

its V-value was 4.729. On the one hand, when the bending diameter is larger than 30 cm, the corresponding bend-dependent modal losses of LP_{11} (<10 dB/m) cannot effectively wear out the amplification of this mode [28], [43]. It is similar to the situation when the bending diameter ranges from 11 cm to 60 cm in the Ref. [43] (the V-value of gain fiber is 5.7735). On the other hand, when the bending diameter decreases, the bend-induced mode coupling becomes serious which means the higher-order mode can be excited and the higher power ratio of the HOMs account for [16] (see Fig. 10). Thus, the irradiance grating (due to the mode interference) becomes stronger, which means that the thermal-introduced refractive index grating is enhanced and the TMI threshold is decreased [9], [47].

Secondly, we found that the IM-FWM threshold can also be suppressed by the increment of bending diameter, which is not revealed in the Ref. [43]. The main reason is that with the decrease of bending diameter, as mentioned above, the bend-induced mode coupling between the LP_{11} mode and LP_{01} mode become serious. Considering the parametric gain [22] of IM-FWM is derived from:

$$g\sqrt{4\gamma^2 P_1 P_2 - (\kappa/2)^2} \tag{3}$$

where, γ is a nonlinear parameter; κ represents the effective phase mismatch, and P1/P2 is the power of LP_{01}/ LP_{11} mode, respectively. Thus, the parametric gain, which is positive related with the product of these two mode powers, is enhanced and the IM-FWM threshold is easier to be reached. As a result, the IM-FWM threshold was improved with the increment of bending diameter in our experiments. Further, the experimental results show that the influence of increasing fiber bending on IM-FWM and TMI is not in the same degree. To be specific, increasing fiber bending has more effects on the latter which threshold incensement is more obvious. Though, the mechanism

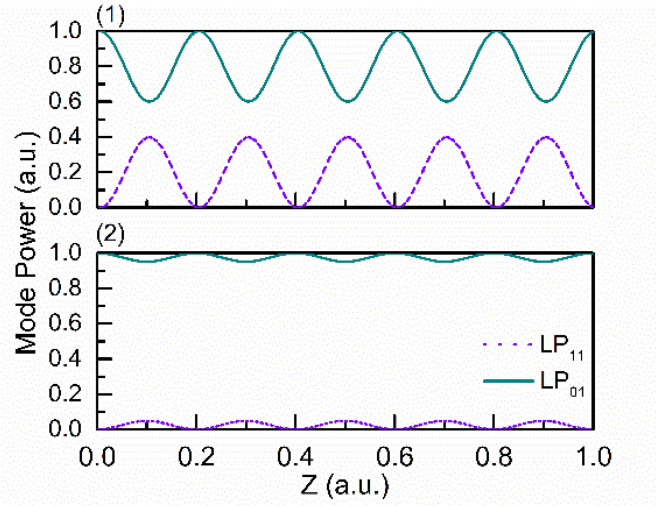

Fig. 10. The schematic diagram of bend-induced mode coupling in different bending diameter. The inset (1) is the situation of small bending diameter and the inset (2) is the situation of large bending diameter.

is not clear, intuitively, it can be understood like that: the parametric gain of IM-FWM is related with product of powers, as mentioned above. In other words, this nonlinear effect happens when absolute intensity of light field is high enough (especially the power of LP_{11} mode), and usually near the end of the amplifier. However, the thermal-induced grating is formed even when the power of LP_{11} mode is weak. It means that the bend-induced coupling affects TMI along the whole fiber. Thus, we believe that the IM-FWM threshold decreases slower than that of TMI, when the bend-induced mode coupling gets serious.

Thirdly, there are still some similarities between TMI and IM-FWM. From Figs. 3(a), 6(a) and 8(b), it can be found that the beam quality increases monotonously with the increment of output power before the presence of TMI or IM-FWM, which represents that the high-order modes (generally the LP_{11} mode) are accumulated. Such increment of M^2 factor can be also observed in the other cases (see Figs. 6(a), 8(b), and 9(b)) before the presence of TMI and IM-FWM. It is implied that the accumulation of high-order mode is indispensable to the result in TMI and IM-FWM. This result is not surprising because TMI and IM-FWM can present only when the LP_{11} mode is strong enough. Notably, the M^2 factor is only 1.08 in the cold cavity (without the pump power) of the amplifier, which shows that the high-order modes should not be induced by the cold cavity but the gain-related effects (e.g., the transverse hole-burning effect [36], the thermally-induced mode coupling [48] and etc.). Furthermore, when the M^2 factor is lower than 1.3, TMI and IM-FWM cannot be observed in our experiments. In fact, to the best of our knowledge, currently, there is no solid experiment observation demonstrating that TMI or IM-FWM can be present with a M^2 factor lower than 1.3 [2], [7]. Therefore, it is inferred that the TMI or IM-FWM should not be present with a M^2 factor lower than 1.3, which can give a condition to estimate whether these two effects should be considered or not. In spite of that, more studies are needed to further validate these inferences.

4. Conclusions

In summary, the TMI and IM-FWM are experimentally studied in the high-power distributed side-pumped amplifier. It is observed that the threshold of TMI and IM-FWM can be very close to each other in our experiments. Then, we investigated the impact of pump scheme on TMI and IM-FWM. Finally, the impact of bending diameter on the above two effects were also studied. We found that the pumping scheme only has a negligible effect on the similarity of two thresholds. Besides, the

counter-pumping scheme is more beneficial to the suppression of both of these two effects, when comparing with co-pumping scheme.

After that, the bending diameter was enlarged from 30 cm to 60 cm, and the pertinent impacts on TMI and IM-FWM were studied. It is found that TMI and IM-FWM can be simultaneously suppressed by increasing the bending diameter. To the best of our knowledge, this is the first demonstration on the positive effect of enlarging bending diameter on suppressing simultaneously both of these two effects. The experimental results also show that the thresholds of two effects are not so close to each other with the 60-cm bending diameter, and the IM-FWM threshold is smaller than that of TMI. Besides, by comparing these thresholds with the M^2 factors, it can also be found that both of these two effects cannot be observed when the M^2 factor is smaller than 1.3, which means that the accumulation of high-order mode is indispensable for the presence of these two effects. We believe that our work can provide some guidance for understanding TMI and IM-FWM in the high-power fiber laser and amplifier.

Acknowledgment

We would like to thank 23th Research institute of China electronic science and technology group for useful help in fabricating the DSCCP fiber, and thank Xiaoming Xi, Zilun Chen, Jinyong Leng, Hu Xiao and Jiawei He for their useful help in experimental studies. The authors would like to thank Dr. Y. Li for proof reading. The authors wish to thank the anonymous reviewers for their valuable suggestions.

References

[1] F. Beier *et al.*, "Experimental investigations on the TMI thresholds of low-NA Yb-doped single-mode fibers," *Opt. Lett.*, vol. 43, pp. 1291–1294, 2018.
[2] K. Shima, S. Ikoma, K. Uchiyama, Y. Takubo, M. Kashiwagi, and D. Tanaka, "5-kW single stage all-fiber Yb-doped single-mode fiber laser for materials processing," *Proc. SPIE*, vol. 10512, p. 105120C, 2018.
[3] M. Ackermann *et al.*, "Extraction of more than 10 kW from a single ytterbium-doped MM-fiber," *presented at the Fiber Lasers XVI: Technology and Systems*, 2019.
[4] H. Zhan *et al.*, "Pump-gain integrated functional laser fiber towards 10 kW-level high-power applications," *Laser Phys. Lett.*, vol. 15, p. 095107, 2018.
[5] E. Stiles, "New developments in IPG fiber laser technology," *presented at the 5th Int. Workshop Fiber Lasers, Dresden, Germany*, 2009.
[6] C. Jauregui, J. Limpert, and A. Tünnermann, "High-power fibre lasers," *Nat. Photonics*, vol. 7, pp. 861–867, 2013.
[7] Tino Eidam *et al.*, "Experimental observations of the threshold-like onset of mode instabilities in high power fiber amplifiers," *Opt. Express*, vol. 19, 2011.
[8] Arlee V. Smith and Jesse J. Smith, "Mode instability in high power fiber amplifiers," *Opt. Express*, vol. 19, 2011.
[9] V. Smith, and J. J. Smith, "Overview of a steady-periodic model of modal instability in fiber amplifiers," *IEEE J. Sel. Top. Quantum Electron.*, vol. 20, pp. 472–483, 2014.
[10] R. Tao, X. Wang, P. Zhou, and Z. Liu, "Seed power dependence of mode instabilities in high power fiber amplifiers," *J. Opt.*, vol. 19, p. 065202, 2017.
[11] S. Naderi, I. Dajani, T. Madden, and C. Robin, "Investigations of modal instabilities in fiber amplifiers through detailed numerical simulations," *Opt. Express*, vol. 21, pp 16111–16129, 2013.
[12] M. Kuznetsov, O. Vershinin, V. Tyrtyshnyy, and O. Antipov, "Low-threshold mode instability in Yb3+-doped few-mode fiber amplifiers," *Opt. Express*, vol. 22, pp. 29714–29725, 2014.
[13] J. J. Smith and A. V. Smith, "Influence of signal bandwidth on mode instability thresholds of fiber amplifiers," *Proc. of SPIE*, vol. 9344, p. 93440L, 2015.
[14] R. Tao, R. Su, P. Ma, X. Wang, and P. Zhou, "Suppressing mode instabilities by optimizing the fiber coiling methods," *Laser Phys. Lett.*, vol. 14, p. 025101, 2017.
[15] V. Smith and J. J. Smith, "Mode instability thresholds of fiber amplifiers," *Proc. of SPIE*, vol. 8601, p. 860108, 2013.
[16] G. Ward, "Maximizing power output from continuous-wave single-frequency fiber amplifiers," *Opt. Lett.*, vol. 40, pp. 542–545, 2015
[17] R. Tao, P. Ma, X. Wang, P. Zhou, and Z. Liu, "Study of wavelength dependence of mode instability based on a semi-analytical model," *IEEE Quantum Electron.*, vol. 51, p. 1600106, 2015.
[18] R. Tao, P. Ma, X. Wang, P. Zhou, and Z. Liu, "Mitigating of modal instabilities in linearly-polarized fiber amplifiers by shifting pump wavelength," *J. Opt.*, vol. 17, p. 045504, 2015.
[19] L. Yin, Z. Han, H. Shen, and R. Zhu, "Suppression of inter-modal four-wave mixing in high-power fiber lasers," *Opt. Express*, vol. 26, pp. 15804–15818, 2018.
[20] W. Liu, W. Kuang, L. Huang, and P. Zhou, "Modeling of the spectral properties of CW Yb-doped fiber amplifier and experimental validation," *Laser Phys. Lett.*, vol. 12, p. 045104, 2015.

[21] G. Kuznetsov, E. V. Podivilov, and S. A. Babin, "Spectral broadening of incoherent nanosecond pulses in a fiber amplifier," *J. Opt. Soc. America B*, vol. 29, pp. 1231–1236, 2012.
[22] G. Agrawal, *Nonlinear Fiber Optics*. Burlington: Elsevier, 2013.
[23] Y. Xiao *et al.*, "Theory of intermodal four-wave mixing with random linear mode coupling in few-mode fibers," *Opt. Express*, vol. 22, no. 26, pp. 32039–32059, 2014.
[24] R. Dupiol *et al.*, "Far-detuned cascaded intermodal four-wave mixing in a multimode fiber," *Opt. Lett.* vol. 42, no. 7, pp. 1293–1296, 2017.
[25] Z. Li *et al.*, "Experimental demonstration of transverse mode instability enhancement by a counter-pumped scheme in a 2 kW all-fiberized laser," *Photon. Res.*, vol. 5, p. 77, 2017.
[26] Q. L. Fang *et al.*, "5 kW near-diffraction-limited and 8 kW high-brightness monolithic continuous wave fiber lasers directly pumped by laser diodes," *IEEE Photon. J.*, vol. 9, 2017, Art. no. 1506107.
[27] T. Li, C. Zha, Y. Sun, Y. Ma, W. Ke, and W. Peng, "3.5 kW bidirectionally pumped narrow-linewidth fiber amplifier seeded by white-noise-source phase-modulated laser," *Laser Phys.*, vol. 28, 2018.
[28] M. J. Li *et al.*, "Limit of effective area for single-mode operation in step-index large mode area laser fibers," *J. Lightwave Technol.*, vol. 27, pp. 3010–3016, 2009.
[29] Z. Huang *et al.*, "A kilowatt all-fiber cascaded amplifier," *IEEE Photon. Technol. Lett.*, vol. 27, pp. 1683–1686, 2015.
[30] H. Chen *et al.*, "Experimental investigations on multi-kilowatt all-fiber distributed side-pumped oscillators," *Laser Phys.*, vol. 29, p. 075103, 2019.
[31] K. H. Yla-Jarkko *et al.*, "Low-noise intelligent cladding-pumped L-band EDFA," *IEEE Photon. Technol. Lett.*, vol. 15, pp. 909–911, 2003.
[32] M. N. Zervas, A. Marshall, and J. Kim, "Effective absorption in cladding-pumped fibers," *Proc. SPIE*, vol. 7914, p. 13, 2011.
[33] V. P. Gapontsev, V. Fomin, and N. Platonov, "Powerful fiber laser system," U.S. Patent 20090092157A1.
[34] M. K. Mikhail, A. B. Igor, M. M. Bubnov, V. S. Aleksei, S. L. Semenov, and M. D. Evgenii, "Pump radiation distribution in multi-element first cladding laser fibres," *Quantum Electron.*, vol. 35, p. 996, 2005.
[35] R. Paschotta, J. Nilsson, A. C. Tropper, and D. C. Hanna, "Ytterbium-doped fiber amplifiers," *IEEE J. Quantum Electron.*, vol. 33, pp. 1049–1056, 1997.
[36] Z. Jiang and J. R. Marciante, "Impact of transverse spatial-hole burning on beam quality in large-mode-area Yb-doped fibers," *J. Opt. Soc. America B*, vol. 25, pp. 247–254, 2008.
[37] C. Jauregui, J. Limpert, and A. Tünnermann, "Derivation of Raman threshold formulas for CW double-clad fiber amplifiers," *Opt. Express*, vol. 17, pp. 8476–8490, 2009.
[38] H. Du, J. Cao, H. Chen, Z. Huang, and J. Chen, "Analytical study on the stimulated Raman scattering threshold in distributed-pumped fiber amplifiers," *Appl. Opt.*, vol. 58, pp. 2010–2020, 2019.
[39] H. Ying, J. Cao, Y. Yu, M. Wang, Z. Wang, and J. Chen, "Raman-noise enhanced stimulated Raman scattering in high-power continuous-wave fiber amplifier," *Optik - Int. J. Light and Electron. Opt.*, vol. 144, pp. 163–171, 2017.
[40] Tao, R. *et al.*, Theoretical study of pump power distribution on modal instabilities in high power fiber amplifiers. *Laser Phys. Lett.*, vol. 14, no. 2, 2017.
[41] Jauregui, C. *et al.*, Optimizing high-power Yb-doped fiber amplifier systems in the presence of transverse mode instabilities. *Opt. Express*, vol. 24, no. 8, pp. 7879–7892, 2016.
[42] J. Li, J. Wang, and F. Jing, "Improvement of coiling mode to suppress higher-order-modes by considering mode coupling for large-mode-area fiber laser," *J. Electromagn. Waves and Appl.*, vol. 24, pp. 1113–1124, 2010.
[43] F. Zhang *et al.*, "Bending diameter dependence of mode instabilities in multimode fiber amplifier," *Laser Phys. Lett.*, vol. 16, p. 035104, 2019.
[44] W. A. Gambling, D. N. Payne, and H. Matsumura, "Mode conversion coefficients in optical fibers," *Appl. Opt.*, vol. 14, pp. 1538–1542, 1975.
[45] L. Palmieri, and A. Galtarossa, "Coupling effects among degenerate modes in multimode optical fibers," *IEEE Photon. J.*, vol. 6, 2014, Art. no. 0600408.
[46] R. Tao, P. Ma, X. Wang, P. Zhou, and Z. Liu, "1.3 kW monolithic linearly polarized single-mode master oscillator power amplifier and strategies for mitigating mode instabilities," *Photon. Res.*, vol. 3, p. 86, 2015.
[47] K. R. Hansen, T. T. Alkeskjold, J. Broeng, and J. Lægsgaard, "Theoretical analysis of mode instability in high-power fiber amplifiers," *Opt. Express*, vol. 21, pp. 1944–1971, 2013.
[48] W. Liu, J. Cao, and J. Chen, "Study on thermal-lens induced mode coupling in step-index large mode area fiber lasers," *Opt. Express*, vol. 27, pp. 9164–9177, 2019